Oxytocin and Vasopressin Involved in Restraint Water-Immersion Stress Mediated by Oxytocin Receptor and Vasopressin 1b Receptor in Rat Brain

Dong-Qin Zhao, Hong-Bin Ai*

Key Laboratory of Animal Resistance of Shandong Province, College of Life Sciences, Shandong Normal University, Shandong Province, People's Republic of China

Abstract

Aims: Vasopressin (AVP) and oxytocin (OT) are considered to be related to gastric functions and the regulation of stress response. The present study was to study the role of vasopressinergic and oxytocinergic neurons during the restraint water-immersion stress.

Methods: Ten male Wistar rats were divided into two groups, control and RWIS for 1h. The brain sections were treated with a dual immunohistochemistry of Fos and oxytocin (OT) or vasopressin (AVP) or OT receptor or AVP 1b receptor ($V_{1b}R$).

Results: (1) Fos-immunoreactive (Fos-IR) neurons dramatically increased in the hypothalamic paraventricular nucleus (PVN), the supraoptic nucleus (SON), the neuclecus of solitary tract (NTS) and motor nucleus of the vagus (DMV) in the RWIS rats; (2) OT-immunoreactive (OT-IR) neurons were mainly observed in the medial magnocellular part of the PVN and the dorsal portion of the SON, while AVP-immunoreactive (AVP-IR) neurons mainly distributed in the magnocellular part of the PVN and the ventral portion of the SON. In the RWIS rats, Fos-IR neurons were indentified in 31% of OT-IR neurons and 40% of AVP-IR neurons in the PVN, while in the SON it represented 28%, 53% respectively; (3) $V_{1b}R$-IR and OTR-IR neurons occupied all portions of the NTS and DMV. In the RWIS rats, more than 10% of OTR-IR and $V_{1b}R$-IR neurons were activated in the DMV, while lower ratio in the NTS.

Conclusion: RWIS activates both oxytocinergic and vasopressinergic neurons in the PVN and SON, which may project to the NTS or DMV mediating the activity of the neurons by OTR and $V_{1b}R$.

Introduction

Restraint water-immersion stress (RWIS) is considered to be a mixture of physical and psychological stressor, and this stimulation in conscious rats induces behavioral responses (anxiety, scrabble, outrage and cry), hypothermia and vagally-mediated gastric hypercontractility, gastric acid hypersecretion and gastric mucosal lesions within a few hours [1–2]. We previously used the model in rats to study the neuronal pathways activated during gastric dysfunction mechanical stimulation. After different durations of RWIS, neuronal activation, demonstrated by Fos-immunoreactivity (Fos-IR), was found significantly increased in specific brain areas, such as the medullary visceral zone [dorsal motor nucleus of the vagus (DMV), nucleus of solitary tract (NTS), area postrema (AP) and nucleus ambiguous (NA)] and the hypothalamus [paraventricular nucleus (PVN) and supraoptic nucleus (SON)] [3–4]. These results suggest the neuronal hyperactivity of the NTS, DMV and AP may be one of the primary central mechanisms of the gastric dysfunctions induced by the RWIS, while the neuronal hyperactivity of PVN and SON may be one of the higher central mechanisms. Brainstem circuits regulating

gastric function have been studied widely [5–7], but little is known about the higher central neuronal mechanisms of the gastric dysfunction induced by the RWIS. Previous studies indicate that the abnormalities of gastric functions induced by RWIS are not due to the hyperactivity of the hypothalamo-pituitary-adrenal (HPA) axis and the sympathetic adrenamedullary system, but due to the hyperactivity of vagal parasympathetic efferents, which largely originating in the DMV and partly in the NA [3,5–9]. It seems that the hyperactivity of the DMV, NTS and AP leads to gastric disfunction. But, our previous researches demonstrated that electrical and chemical stimulations of the DMV and NA inhibited gastric motility [10–11]. So, whether the hyperactivity of the higher centre of the anterior hypothalamus relieves the inhibition of gastric motility mediated by the primary nerve centre during the RWIS? If so, what are the neurotransmitters released by the anterior hypothalamus neurons?

The PVN and SON are the main nuclei of the anterior hypothalamus, which might be stimulus-dependent [8,12]. While the SON is composed exclusively of magnocellular neurons, the PVN is more heterogeneous and includes also parvocellular neurons [13]. The parvocellular region of the PVN, based on the

cell density and cell size, can be divided into the anterior (PaAP), medial (PaMP), posterior (PaPo) and periventricular (Pe) subdivisions. The magnocellular region of the PVN is characterized by the compact clustering of the large cells and can be divided into lateral (PaLM) and medial (PaMM) subdivisions [14]. Vasopressin (AVP) and oxytocin (OT) are two structurally related nonapeptides synthesized mainly in the magnocellular neurons of the PVN and SON [15–17], and may act as neurotransmitters and/or neuromodulators which are considered to be related to gastric functions [18] and the regulation of stress response [19–27]. One aim of the present study was to find out whether the activated neurons in the PVN and SON of rats induced by RWIS were OT and AVP neurons.

Furthermore, to illustrate the OT and AVP neurons in the anterior hypothalamus taking part in the mediation of signals induced by RWIS, the other aim of this study was to determine whether the phenotypic nature of activated neurons in the medullary visceral zone were AVP sensitive or OT sensitive neurons, where AVP or OT receptors located. To date, three types of AVP receptors have been described: V_{1a}, V_{1b} and V_2 receptors, whereas OT receptors only one [28–30]. Receptors for OT and AVP have been found in various regions of the rat brain, including the hypothalamic nuclei, NTS, DMV and so on [29–32]. In the central nervous system, the action of AVP seems to be predominantly mediated by V_1-type AVP receptors [33–34].

So, in the present study, the extent of activation as well as the distribution of the activated neurons, mainly in PVN, SON, DMV and NTS, was determined by immunohistochemistry employing an antiserum specific for Fos protein, which is known as a marker of neural activation [35]. To evaluate the role of OT and AVP during the RWIS, the phenotype nature of activated neurons was determined by a double immunohistochemical method for co-locations of Fos with either AVP, OT, $V_{1b}R$ or OTR specific antibodies.

Materials and Methods

Preparation of animals

Male Wistar rats (Experimental Animal Center of Shandong University, Jinan, China), weighing 180–200 g, were housed two per cage at an ambient temperature of $22\pm2°C$ under a normal day/night cycle with foot and water available ad libitum before initiation of the RWIS. Experiments were initiated at least 7 days after arrival. Before stress, the rats were fasted for 24 hours, but allowed free access to water.

Stress protocols

Ten rats were randomly divided into two groups in accordance with the duration of RWIS, respectively: the RWIS group and the control group. RWIS was performed as previously described [36]. Briefly, under light ether anesthesia, the four limbs of each rat in the stressed group were bounded gently but securely on a wooden board by use of medical adhesive tape. When the rats were conscious, they were vertically immersed in water $(21\pm1°C)$ to the level of the xiphoid for 1 h. Unstressed rats, as a control group, were not stressed but were otherwise under identical conditions. To avoid the effect of diurnal variations on the Fos expression, the experiment was performed between 9:00 and 11:00 a.m. All procedures were performed in accordance with the ethic guidelines of the International Association for the Study of Pain [37].

Tissue processing

At the end of the procedure, the rats were deeply anesthetized by intraperitoneal injections of over sodium pentobarbital (100 mg/kg body weight) and perfused via the ascending aorta

with 200 ml 0.01 mol/L phosphate buffered saline (PBS, pH 7.4) followed by 500 ml 4% paraformaldehyde, 0.1% glutaraldehyde and 14% saturated picric acid in 0.1 mol/L phosphate buffer (pH 7.4). After perfusion, the brain was removed and post-fixed at $4°C$ for 4 h in the same fixative, and then infiltrate with 20% sucrose in 0.1 mol/L phosphate buffer for 48 h at $4°C$. Series of frozen coronal sections of the hypothalamus and medullary visceral zone were cut at 30 µm in a cryostat and collected into 0.01 mol/L PBS.

Immunohistochemistry

The immunoreaction of Fos plus neuropeptide, AVP and OT, and their receptor, V1b and OTR, was detected by a dual SP (streptavidin-biotin-peroxidase) immunohistochemical technique. Briefly: (1) Free floating sections were rinsed in 0.01 mol/L PBS followed by a preincubation in methanolic 3% H_2O_2 for 30 min at room temperature to eliminate endogenous peroxidase activity. (2) After rinsing in 0.01 mol/L PBS, the sections were incubated with blocking buffer, containing 5% normal goat serum and 0.3% Triton X-100 in 0.01 mol/LPBS for 30 min, and then were incubated with rabbit anti-c-Fos antibody (sc-52, Santa Cruz Biotechnology Inc, USA), diluted 1:2000 in 0.01 mol/L PBS containing 3% normal goat serum (NGS) and 0.3% TritonX-100 for 24 hours at $4°C$. (3) At the end of this incubation period, rinsing in 0.01 mol/L PBS, the sections were incubated with the biotinylated goat anti-rabbit IgG (Zymed Laboratories Inc, USA) for 1 h at room temperature and next PBS rinse were followed by incubation with streptavidin-biotin-horseradish peroxidase complex (Zymed Laboratories Inc, USA) for 1 h at room temperature. (4) After several rinsing in PBS, the sections were submitted to a diaminobenzidine hydrochloride (DAB, Sigma Chemical Co. St Louis, MO, USA), intensified with 0.05% cobalt chloride and 0.05% nickel ammonium sulfate for 4–5 min. This method produces a blue-black nuclear reaction product. (5) The Fos-immunoreactive (Fos-IR) sections were rinsed and incubated for 24 h with rabbit anti-AVP (1:2000, Abcam plc 332 Cambridge Science Park, Cambridge, CB4 0WN, UK), mouse anti-OT (1:2000, Abcam plc 330 Cambridge Science Park, Cambridge, CB4 0FL, UK), rabbit anti-$V_{1b}R$ (1:200, International Laboratory USA) or anti-OTR (1:200, USCNLIFE Science CO, USA) in 3% NGS and 0.3% TritonX-100 for 48 hours at $4°C$. (6) and (7) were the same as (3) and (4). (8) The visualization of the immunoreactive products was obtained by reaction with unintensified DAB that produces a brown reaction product. (9) Lastly, the free-floating sections were mounted on gelatin-coated glass slides, air-dried overnight, dehydrated in a series of alcohols, cleared in xylene and placed under a coverslip with Permount.

Evaluation of immunostaining

Pictures of brain sections were taken under identical conditions with a BX51 Olympus microscope (Olympus Corporation, Japan) coupled to an Olympus DP70 camera. The nomenclature and nuclear boundaries defined in the rat brain stereotaxic atlas of Paxinos & Watson [38] were used in this study. For quantitative assessment, the number of immunoreactive neurons using Image-Pro Plus 6.0 (Media Cybernetics Inc, USA), was counted at three levels. For the PVN: the anterior portion (Bregma, -1.08 to -1.32 mm), the medial portion (-1.72 to -1.92 mm), and the posterior portion (Bregma, -2.04 to -2.16 mm). For the NTS and DMV: rostral (Bregma, -12.96 to -13.32 mm), intermediate (Bregma, -13.80 to -14.04 mm), and caudal (Bregma, -14.52 to -14.76 mm) [7]. The immunoreactive neurons in SON were counted at one level (Bregma, -0.92 to -1.44 mm). In each nucleus, 3 kinds of neurons were counted, which were Fos-IR

nuclei, AVP or OT or $V_{1b}R$ or OTR-IR neurons and Fos+ AVP or OT or $V_{1b}R$ or OTR -IR neurons.

The number of immunoreactive neurons was counted in three near sections per animal and the average values of them in 0.01 mm^2 are reported as the number of immunoreactivity.

Statistical analysis

Counting was performed in five rats for each condition and the data obtained from each animal were used to calculate group means ±SEM. The statistical procedures were performed with SPSS13.0 software (SPSS, Chicago, IL, USA). Statistical analysis about data in different portions of the PVN, NTS and DMV were performed by two-way analysis of variance (ANOVA) followed by S-N-K's *post hoc* test individually. Statistical analysis about data in the SON was performed by Student's *t*-test. $P<0.05$ and $P<0.01$ were considered statistically significant.

Results

RWIS induced Fos expression in specific brain nuclei

Changes in neural activity were assessed by monitoring Fos expression in the hypothalamus and the medullary visceral zone after RWIS for 1 h. The response to RWIS and the pattern of distribution of Fos-IR were essentially the same as previously reported by us, while few Fos-IR neurons appeared in the same area in unstressed rats [3]. Briefly, the activated neurons mainly occupied the anterior hypothalamus, including the PVN and SON, and the medullary visceral zone, including the NTS and DMV. SO, in the present study, we focused on the hypothalamic areas containing large populations of vasopressinergic, oxytocinergic neurons responsive to RWIS and medullarry areas containing the AVP or OT sensitive neurons responsive to RWIS.

Distribution of Fos and Fos+OT and Fos+AVP immunoreactive neurons in the hypothalamus

PVN. RWIS for 1 h increased Fos-IR nuclei to 7.9±1.3 (cells per 0.01 mm^2) in the PVN compared with 3.3±0.3 in unstressed rats, *i.e.* 2.4-fold ($P<0.01$) (Figure 1). Maximal number of Fos-IR neuclei were observed in the medial portion in the PVN, while comparably less of them was present in its anterior and posterior portions, the difference was significant ($F_{2,12}=53.913$, $P=0.000$). Numerous Fos-IR nuclei occurred explicitly in the PaMP, PaMM and PaLM. Fos-IR nuclei in the PaMP were heterogeneous in size and had irregular profiles, while those in the PaLM were large round and more homogeneous in size. Besides these locations, some Fos-IR neurons were also found in the lateral portion of the PaAP, the dorsal cap (PaDC), ventral (PaV) subdivisions of the PVN. Similarly, a few of Fos-IR neurons were observed in the Pe and PaPo (Figure 2).

OT-IR neurons within the PVN were mostly located in the medial portion, including the PaMM, where they aggregated into a compact cell cluster, and the PaLM, where they had fusiform or round profiles with number of neuronal processes (Figure 2). Besides these locations, the lateral portion of the PaAP, the PaDC and PaV had a moderate number of OT-IR neurons and a few were scattered in the PaMP, PaPo and Pe, where closed to the wall of the third ventricle (Figure 2). Fos+OT-IR neurons in the PVN were mainly located in the PaMM, PaLM and the PaV, and to a less extent, in the lateral portion of the PaAP, PaDC and PaMP. In the PaPo almost no double staining cells were found. Overall, in the PVN, Fos+OT-IR neurons represented in 31.40%±0.76% of total OT-IR neurons in the RWIS group, and had significant difference compared with 11.74%±3.71% in the control group ($P<0.01$).
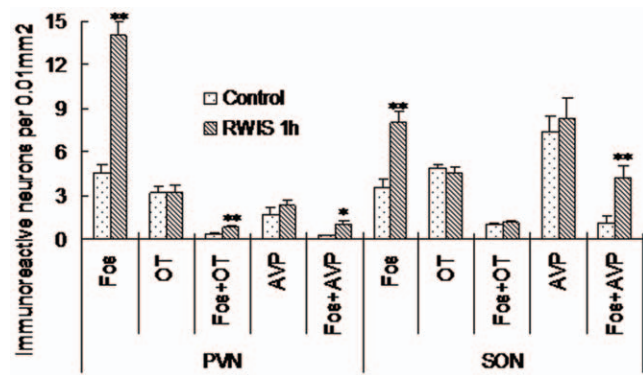
Figure 1. Cells count (cells per 0.01 mm^2) of Fos-IR and OT-IR or AVP-IR neurons in the PVN and SON. n = 5 rats per group. Each group represents mean±SEM. ** $P<0.01$, * $P<0.05$ *vs* the control group.
doi:10.1371/journal.pone.0023362.g001

AVP-IR neurons mainly located in the magnocellular portion of the medial part of the PVN, including the PaMM and the PaLM, where most of Fos+AVP-IR neurons were observed (Figure 3). In the PaMP, PaDC as well as the PaPo, only scattered AVP-IR neurons were found, and almost no AVP-IR neurons located in the anterior portion of the PVN and the Pe (Figure 3). Fos+AVP-IR neurons in response to RWIS represented in 40.39%±6.78% of AVP-IR neurons while 14.21%±3.42% in the control group ($P<0.01$).

SON. Likewise in the case of Fos-IR nuclei in the PVN, the number of Fos-IR nuclei in the SON in the RWIS group (8.0±0.8 cells per 0.01 mm^2) was significantly higher than that in the control group (3.5±0.6 cells per 0.01 mm^2) ($P<0.01$) (Figure 1). In contrast to the PVN, Fos-IR nuclei in the SON were less abundant and evenly distributed. Morphometry showed that Fos-IR nuclei in the SON were large and round in similar size (Figure 4).

OT-IR neurons were observed mainly in dorsal part of the SON (Figure 4 A,B). Fos+OT-IR neurons in response to RWIS represented in 27.94%±3.05% of OT-IR neurons and 19.62%±2.88% in the control group ($P<0.05$).

Compared with the OT-IR neurons, AVP-IR neurons were mainly distributed in the ventral part of the SON (Figure 4 C,D). The percentage of Fos+AVP-IR in the total AVP-IR neurons in the RWIS rats was significantly increased by RWIS for 1 h (52.88%±4.53%) compared with that in the unstressed rats (19.44%±8.88%) ($P<0.01$).

Distribution of Fos and Fos+OTR and Fos+$V_{1b}R$ immunoreactive neurons in the medullary visceral zone

DMV. In the DMV, RWIS for 1 h induced a robust increase in Fos-IR nuclei by 4.2 times (2.1±0.5 *vs* 0.5±0.2 in the control group, cells per 0.01 mm^2) ($P<0.01$) (Figure 5). The labeled neuronal nuclei in the DMV were large and round in similar size (Figure 6,7). The occurrence of Fos-IR nuclei was evident from the rostral to the caudal portions of the DMV. Maximal number of Fos-IR neuclei were found in the intermediate part of the DMV, while comparably less of them was present in its anterior and posterior portions, the difference was significant ($F_{2,12}=5.907$, $P=0.015$).

OTR-IR neurons were observed evidently from the rostral to the caudal portions of the DMV either in the RWIS rats or the unstressed rats (Figure 6). OTR-IR neurons in the DMV, evenly distributed, were large fusiform or round profiles with few number of neuronal processes. The major location of Fos+OTR-IR neurons was the intermediate part of the DMV, and less of
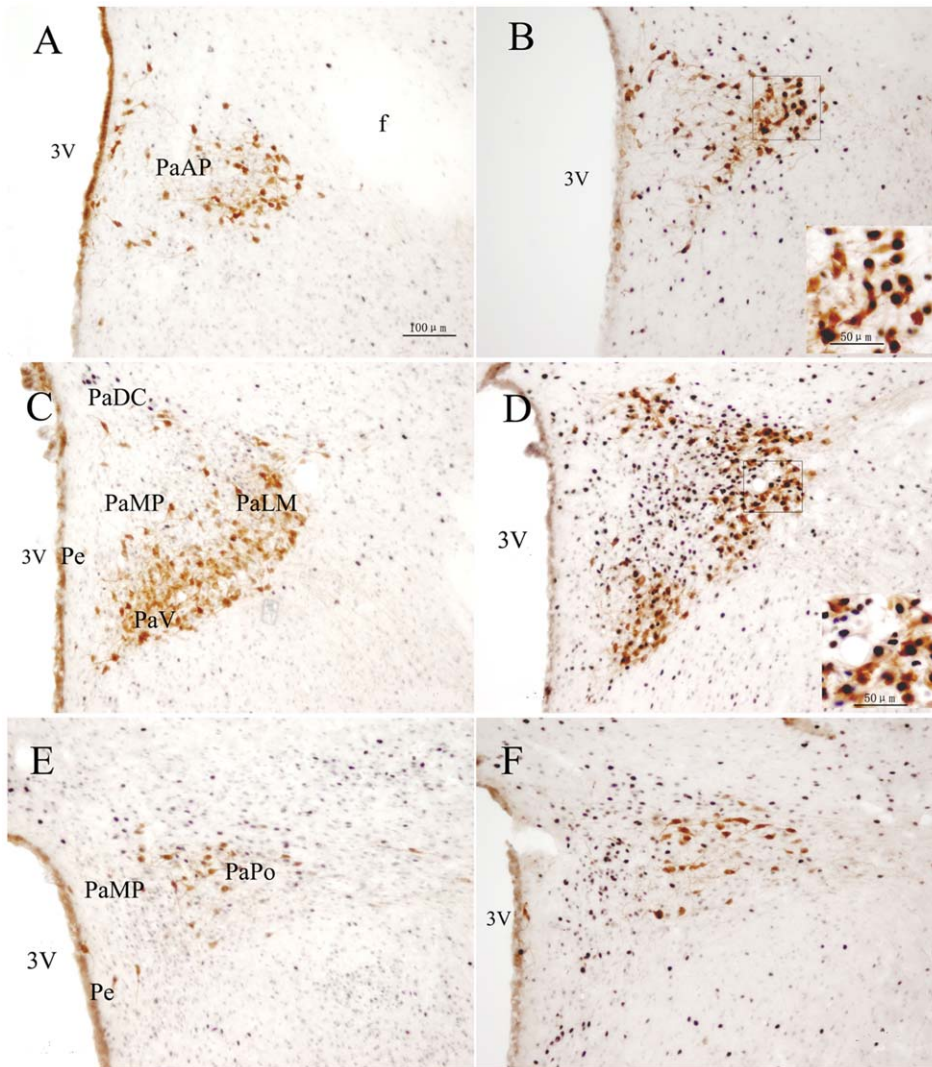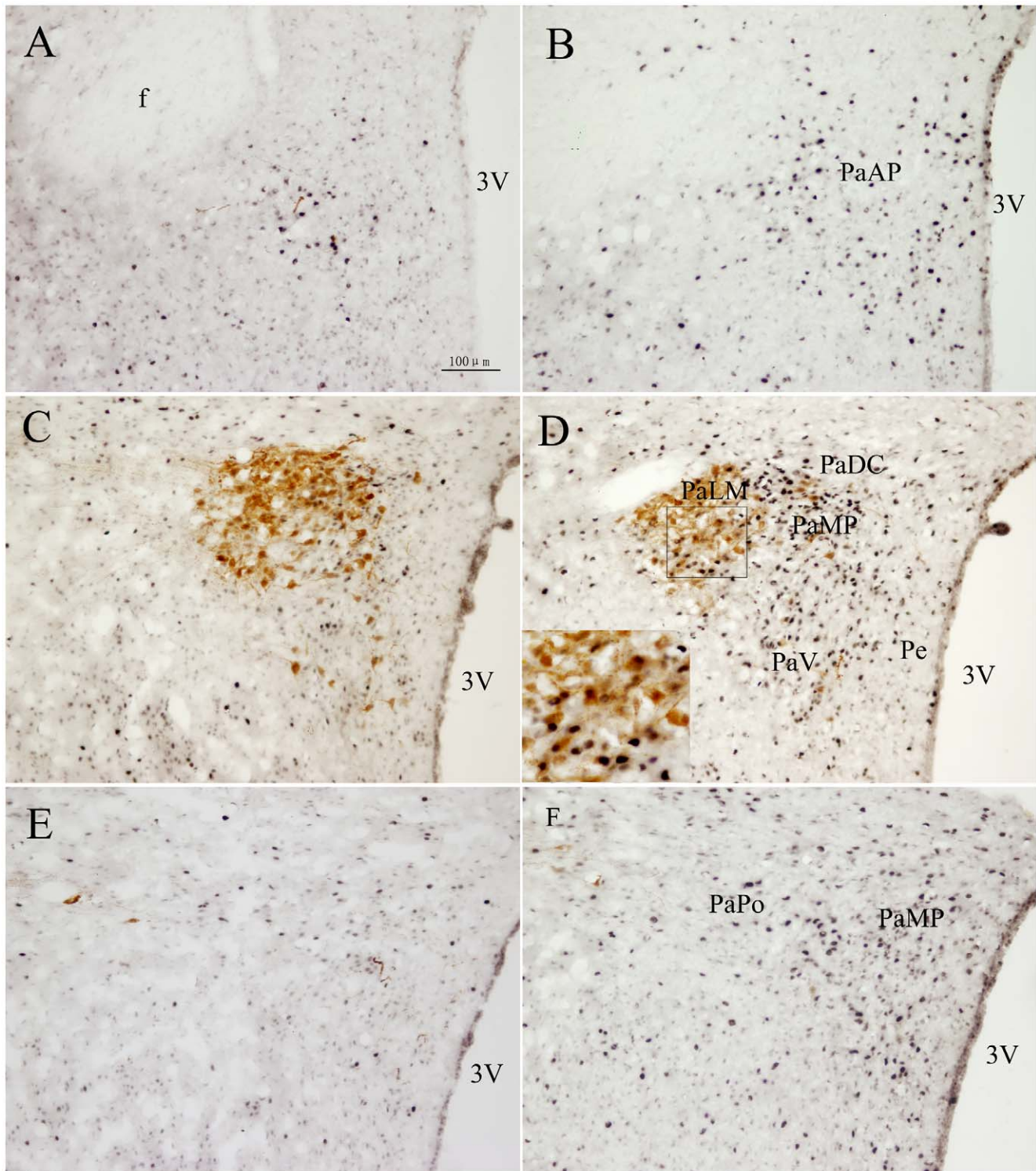
Figure 2. Double immunohistochemical staining of Fos-IR and OT-IR neurons in the PVN. A, B: the anterior. C, D: the medial. E, F: the posterior. A, C, E: the unstressed rats. B, D, F: rats induced by restraint water-immersion stress for 1 h. The inserts show a higher magnification (400X) of cells in the small boxes. PaAP: anterior parvicellular part of the PVN; PaLM: lateral magnocellular part of the PVN; PaV: the ventral part of the PVN; PaMP: medial parvocellular part of the PVN; PaDC: dorsal cap of the PVN; Pe: periventricular of the PVN; 3V: 3rd ventricle. Bar in all panels is 100 µm, while in the inserts is 50 µm.
doi:10.1371/journal.pone.0023362.g002

them was present in its posterior and anterior portions, but the difference was not significant ($F_{2,12} = 0.845$, $P = 0.454$). Overall, in the DMV, Fos+OTR-IR neurons represented in $10.22\% \pm 0.54\%$ of total OTR-IR neurons in the RWIS group, and compared with that in the control group ($2.87\% \pm 0.34\%$), the difference was significant ($P < 0.01$).

V_{1b}R-IR neurons were also observed evidently from the rostral to the caudal portions of the DMV either in the RWIS rats or the unstressed rats (Figure 7). Compared with OTR-IR neurons, V_{1b}R-IR neurons in the DMV were lesser in size and round profiles without any neuronal processes. The major location of Fos+V_{1b}R-IR neurons was the intermediate part of the DMV, while less of them was present in its anterior and posterior portions, the difference was significant ($F_{2,12} = 5.735$, $P = 0.018$). Overall, in the DMV, Fos+V_{1b}R-IR neurons represented in $10.72\% \pm 3.22\%$ of total V_{1b}R-IR neurons, compared with $2.87\% \pm 1.77\%$ in the control group, the difference was significant ($P < 0.05$).

NTS. In the NTS, there was an induction of Fos-IR nuclei in RWIS rats when compared with unstressed rats (2.1 ± 0.1 vs 0.8 ± 0.1 cells per 0.01 mm^2, $P < 0.01$) (Figure 5). The location of Fos-IR nuclei was evident from the rostral to the caudal portions of the NTS (Figure 6,7). There was no significant difference in the number of Fos-IR nuclei in any portion of the NTS, in spite of the occurrence of Fos-IR nuclei in the rostral and caudal portions being less numerous ($F = 1.339$, $P > 0.05$). Fos-IR nuclei were mainly observed in the intermediate (imNTS) and ventrolateral (vlNTS) (Figure 6,7), along with a few stained cells were found in the ventral (vNTS) and the medial (mNTS) subnuclei.
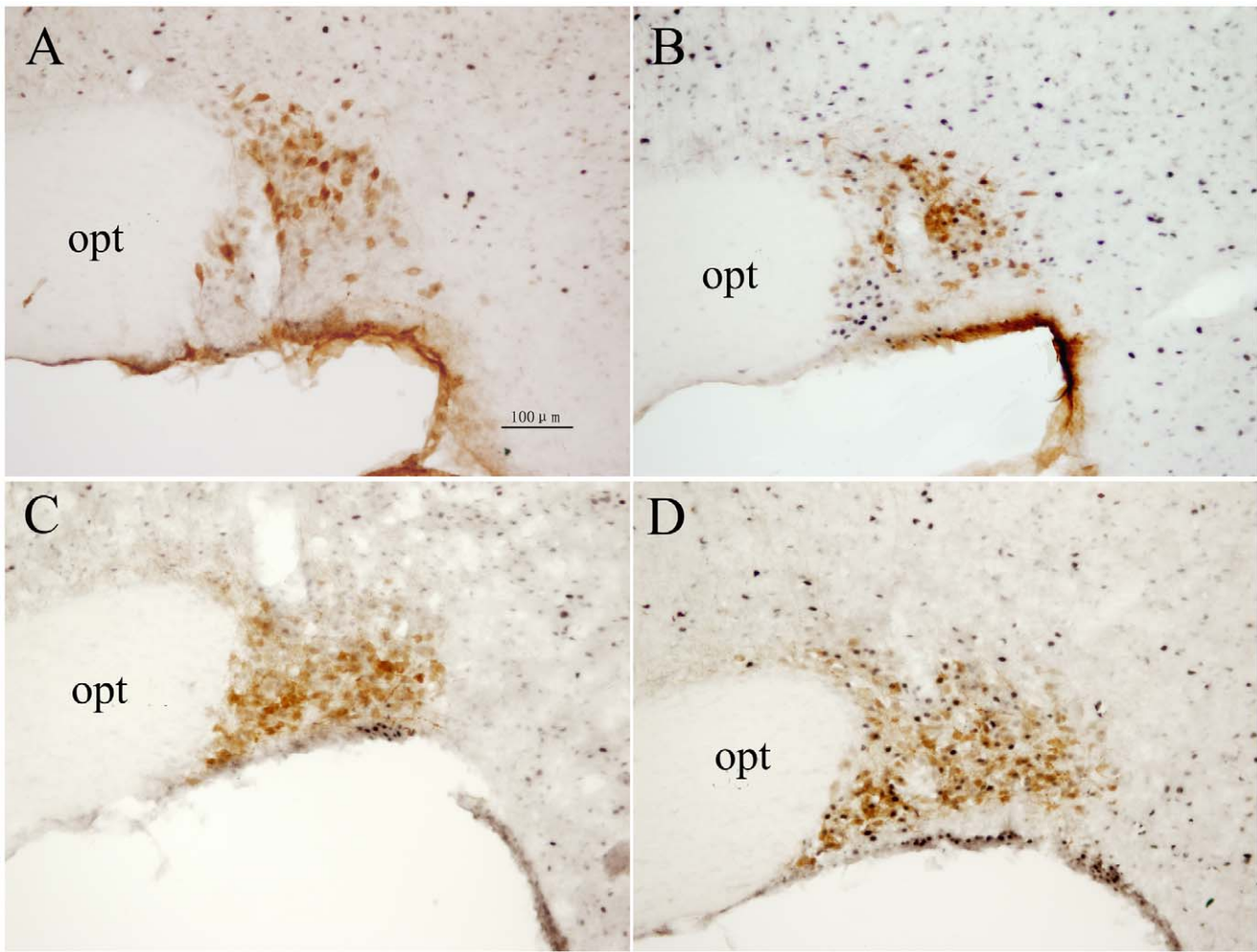
OTR-IR neurons were observed evidently from the rostral to the caudal portions of the NTS either in the RWIS rats or the unstressed rats (Figure 6). Compared with the DMV, in the NTS, OTR-IR neurons, mainly located in the mNTS, imNTS and vNTS, were fusiform or round profiles without any neuronal processes, and smaller in size with a scanty cytoplasm that was

Figure 3. Double immunohistochemical staining of Fos-IR and AVP-IR neurons in the PVN. A, B: the anterior. C, D: the medial. E, F: the posterior. A, C, E: the unstressed rats. B, D, F: rats induced by restraint water-immersion stress for 1 h. The inserts show a higher magnification (400X) of cells in the small boxes. The portions of the PVN was same as Figure2. 3V: 3rd ventricle. Bar in all panels is 100 μm, while in the inserts is 50 μm.
doi:10.1371/journal.pone.0023362.g003

hardly distinguished in double immunostained neurons. The major location of Fos+OTR-IR neurons was the intermediate part of the NTS, and less of them was present in its posterior and anterior portions, but the difference was't significant ($F_{2,12} = 0.336$, $P = 0.721$). Within the NTS, most of Fos+OTR-IR neurons were confined to the imNTS and vNTS. Overall, in the NTS, Fos+OTR-IR neurons represented in $9.79\% \pm 0.96\%$ of total OTR-IR neurons in the RWIS group, and compared with $5.25\% \pm 0.09\%$ in the control group, the difference was significant ($P < 0.01$).

Figure 4. Double immunohistochemical staining of Fos-IR and OT-IR or AVP-IR neurons in the SON. A, C: the unstressed rats. A, B: OT-IR. C, D: AVP-IR. B, D: rats induced by restraint water-immersion stress for 1 h. OT-IR neurons were observed mainly in dorsal part of the SON, while AVP-IR neurons were mainly distributed in the ventral part of the SON. opt: optic tract. Bar in all panels is 100 μm.
doi:10.1371/journal.pone.0023362.g004

$V_{1b}R$-IR neurons located evidently from the rostral to the caudal portions of the NTS either in the RWIS rats or the unstressed rats (Figure 7). The profile and distribution of $V_{1b}R$-IR
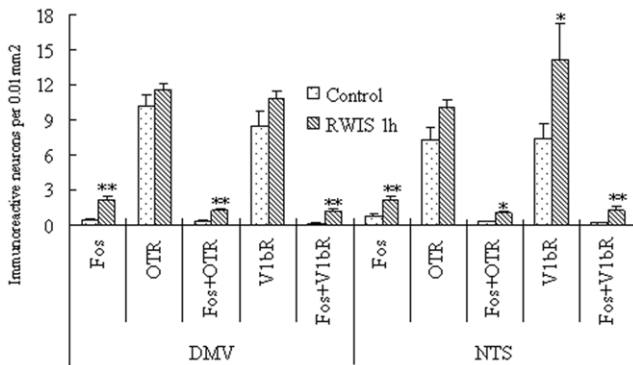

Figure 5. Cells count (cells per 0.01 mm²) of Fos-IR and OTR-IR or $V_{1b}R$-IR neurons in the DMV and NTS. n = 5 rats per group. Each group represents mean±SEM. ** $P<0.01$, * $P<0.05$ vs the control group.
doi:10.1371/journal.pone.0023362.g005

neurons were similar with OTR-IR neurons. The location of Fos+$V_{1b}R$-IR neurons was even within the different portions of the NTS ($F_{2,12}=0.059$, $P=0.943$). Within the NTS, most of Fos+$V_{1b}R$-IR neurons were confined to the imNTS and dlNTS. Overall, in the NTS, Fos+$V_{1b}R$-IR neurons represented in 8.16%±0.82% of total $V_{1b}R$-IR neurons in the RWIS group, and compared with that in the control group (3.57%±0.38%), the difference was significant ($P<0.01$). Furthermore, there was significant difference in the percentage of Fos+$V_{1b}R$-IR neurons of the Fos-IR nuclei between the RWIS group (49.43%±3.36%) and the control group (27.03±2.91%) ($P<0.01$).

Discussion

In the present study, RWIS for 1 h evoked a marked neuronal activation in the SON, PVN, DMV and NTS, a pattern consistent with that reported previously by us under similar conditions [3]. The characterizations of these activated neurons in the PVN, SON, DMV and NTS were assessed by bouble-staining. Morphological aspects and chemical coding revealed that the RWIS activates the hypothalamic oxytocinergic and vasopressinergic neurons and these neurons may project to the NTS and DMV mediated by OTR and $V_{1b}R$.
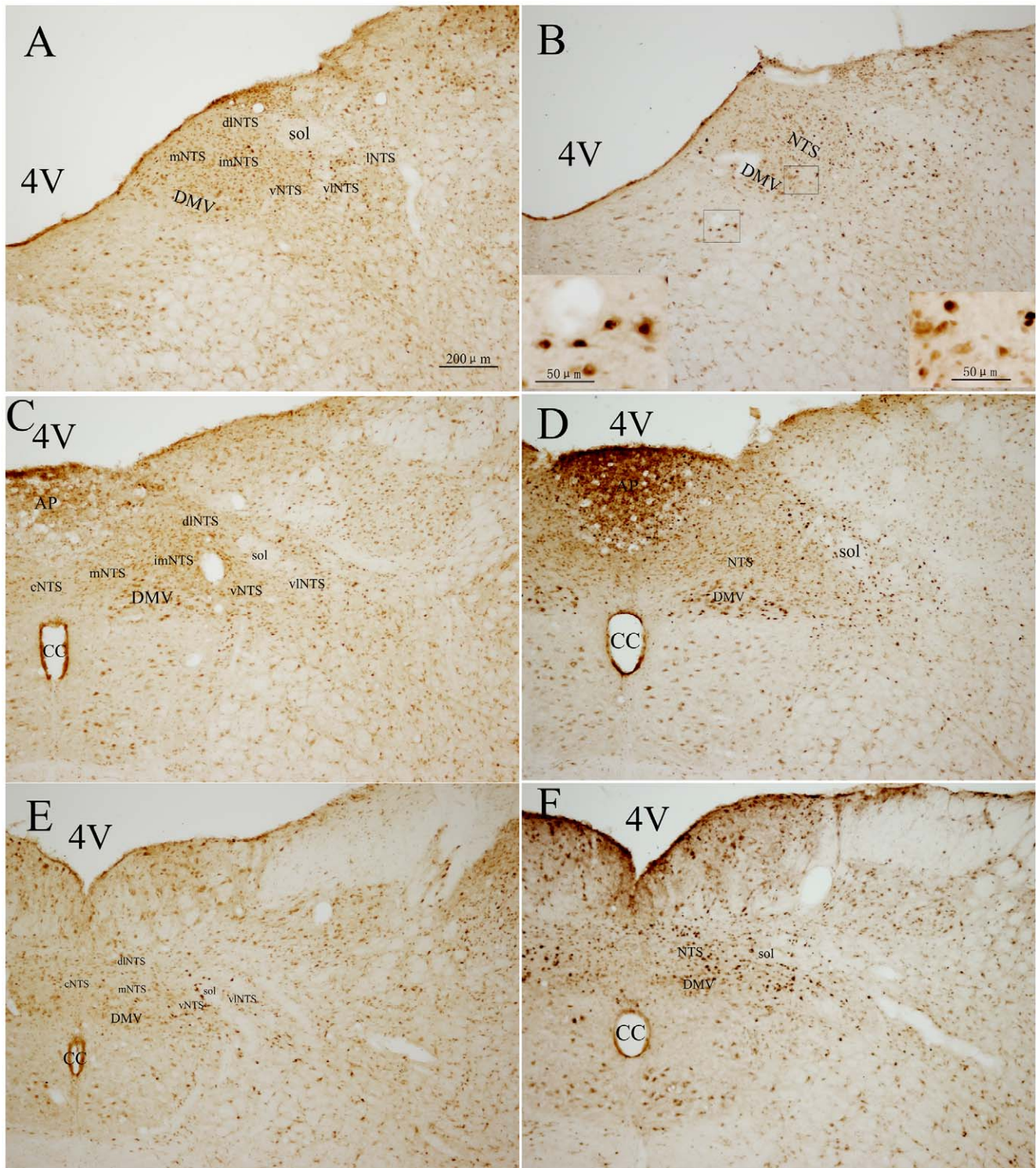
Figure 6. Double immunohistochemical staining of Fos-IR and OTR-IR neurons in the DMV and NTS. A, B: rostral. C, D: intermediate. E, F: caudal. A, C, E: Unstressed rats. B, D, F: rats induced by restraint water-immersion stress for 1 h. The inserts show a higher magnification (400X) of cells in the small boxes. cNTS: commissural nucleus of solitary tract; mNTS: medial nucleus of solitary tract; imNTS: intermediate nucleus of solitary tract; vNTS: ventral nucleus of solitary tract; vlNTS: ventrolateral nucleus of solitary tract; dlNTS: dorsolateral nucleus of solitary tract; 4V: 4rd ventricle; CC: central canal. Bar in all panels is 100 µm, while in the inserts is 50 µm.
doi:10.1371/journal.pone.0023362.g006
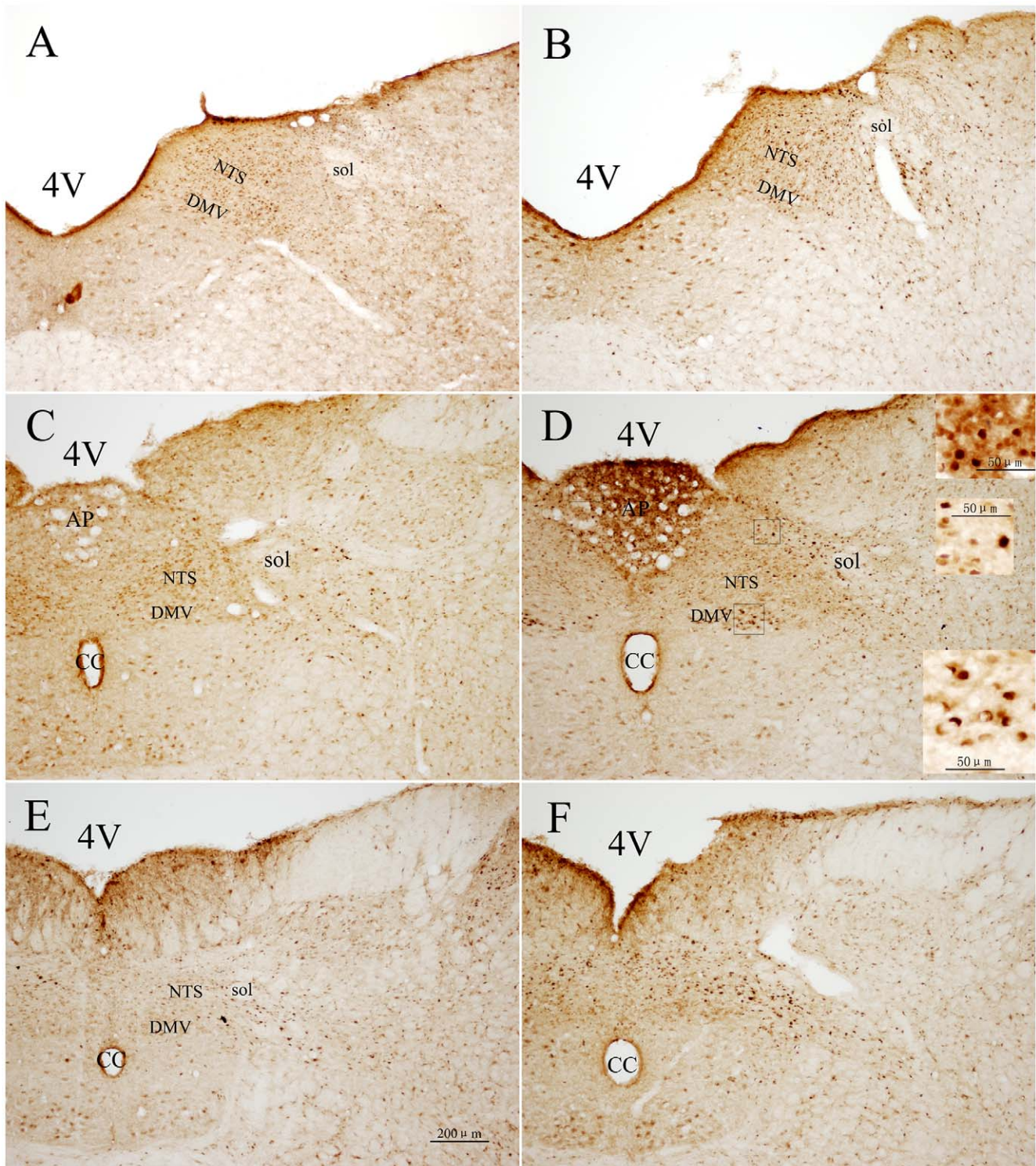
Figure 7. Double immunohistochemical staining of Fos-IR and V_{1b}R-IR neurons in the the DMV and NTS. A, B: rostral. C, D: intermediate. E, F: caudal. A, C, E: Unstressed rats. B, D, F: rats induced by restraint water-immersion stress for 1 h. The inserts show a higher magnification (400X) of cells in the small boxes. The subdivision of the NTS was same as Figure 6. 4V: 4rd ventricle; CC: central canal. Bar in all panels is 100 μm, while in the inserts is 50 μm.
doi:10.1371/journal.pone.0023362.g007

Oxytocinergic and Vasopressinergic hypothalamic neurons involved in the mediation of signals induced by RWIS

PVN and SON, as the main nuclei of the anterior hypothalamus, not only innervate areas of the brain known to be involved in cardiovascular regulation, but might be stimulus-dependent a variety of stimuli [19-26,39-40]. In the present study, the marked activation of neurons induced by RWIS encompasses mainly the SON and PVN, which accounts for the important role of the anterior hypothalamus in response to the RWIS. Furthermore, the pattern emerging from the results of immunohistochemistry revealed a topographically distinct distribution of activated neurons in the subdivisions of the PVN and in the SON. In the SON Fos-IR nuclei were evenly distributed, while in the PVN, the PaMP, PaLM and PaMM subdivisions showed a robust increase in Fos-IR nuclei, the PaAP, PaDC and PaV subdivisions displayed a modest Fos expression, and only a few of Fos-IR nuclei scattered in the Pe and PaPo. This suggests that different subdivisions of the PVN may take a different role in this response and the PVN may be involved in the regulation of a variety of central neural functions.

Swanson LW and Sawchenko PE reported that OT-containing neurons are massed in the central core of the posterior magnocellular subdivision of the PVN and the dosolateral part of the SON, while AVP are massed in the circumference of the PVN and the ventromedial portion of the SON [41]. In the present study, OT-IR and AVP-IR neurons mostly located in the medial portion of the PVN, including PaMM and PaLM, but in the SON the OT-IR neurons mainly located in the dorsal part, while AVP-IR evenly distributed within the SON. The distribution of the OT- and AVP-IR perikarya in the PVN and SON co-responded well with the principal distribution of OT- and AVP-IR neurons reported in other rats or mice studies [25–27]. Double labeling showed that the majority of oxytocinergic and vasopressinergic neurons in the hypothalamus, including the PVN and SON, expressed Fos, which indicated that these neurons were directly or indirectly activated by the RWIS. In the PVN, Fos-IR nuclei were indentified in 31% of OT-IR and 40% of AVP-IR neurons, while in the SON it represented 28% of OT-IR and 53% of AVP-IR neurons. These findings indicate that PVN oxytocinergic and vasopressinergic neurons are all prominently activated by the RWIS, and vasopressinergic neurons in the SON are key component in the integration of stress-related signals, while oxytocinergic neurons seem to participated to a less extent. The different OT and AVP ratio in the neuroendocrine activation of the PVN and SON expends previous studies showing a differential activation of oxytocinergic and AVP-IR neurons in response to a variety of stimuli. For example, proximal colon distension induced Fos expression in about 81% of OT-containing neurons and 18% of vasopressin neurons in the PVN, while in the SON 36% and 16%, respectively [27]. Osmotic stress activated 38%-45% of the oxytocinergic and 62%-67% of the vasopressinergic neurons in the PVN, and more than 50% of oxytocinergic and vasopressinergic neurons in the SON, while immobilization stress induced Fos expression in only 4%-8% of the oxytocinergic neurons and 10%-15% of the vasopressinergic neurons in the PVN, and less than 4% of oxytocinergic and vasopressinergic neurons in the SON [26]. These observations and the present results suggest that activations of oxytocinergic and vasopressinergic neurons in the PVN and SON depends on the style of stressors and that the hypothalamic oxytocinergic and vasopressinergic neurons may be involved in the regulation of a variety of central neural functions.

Oxytocin-sensitive and Vasopressin-sensitive neurons in the medullary visceral zone involved in the mediation of signals induced by RWIS

The NTS is the major recipient of visceral afferent information arising from various regions of the gastrointestinal tract, while the DMV is a visceral motor nucleus, and morphometry showed that the vagal parasympathetic neurons innervating the stomach are largely located in the DMV [42–44]. RWIS for 1 h induced a robust increase in Fos-IR nuclei in the NTS and DMV, which indicated that the NTS and DMV neurons were responsive to the RWIS. These results are in good agreement with our previous reports that RWIS induced the expression of Fos protein in the NTS and DMV [3–4]. The difference of the activated neurons in different portions of the NTS and DMV may be due to their different roles in modulating the gastric functions during RWIS [3,6–7,45–46].

Previous studies found that OT and AVP neurons in the PVN project to the NTS, DMV and spinal cord at the level of sympathetic preganglionic neurons, where OT and V1 receptors are present [11,28,47]. In the present study, more than 10% of OTR-IR and V_{1b}R-IR neurons in the DMV were activated in the RWIS rats while less than 3% in the unstressed rats. In the NTS, the percentages of Fos-IR neurons in the OTR-IR and V_{1b}R-IR neurons were 10% and 8%, while 5% and 3% in the unstressed rats, respectively. The significant difference of the ratio between the RWIS and unstressed groups indicates that the OT-sensitive and AVP-sensitive neurons may be involved in the modulation of the gastric dysfunction during the RWIS. But, there was no difference in the number of Fos+OTR or V_{1b}R double-labeled neurons in any portions of the DMV and NTS. This result may suggest that OT or AVP-containing neurons are involved in the regulation of a variety of central neural functions. Oxytocinergic and vasopressinergic neurons in the PVN and SON receive afferent projections from visceral centers, and then release AVP or OT, which have been shown to stimulate autonomic neurons in the NTS and DMV, thereby improving vagal outflow and augmenting reflex [48–50]. Microinjection of OT into the rat DVC activates gastric projecting neurons in the NTS and DMV [18], and inhibits gastric motility [51]. Moreover, the decrease in gastric motility in response to PVN stimulation is blocked by microinjection of OT receptor antagonists in the DMV [51].

Oxytocinergic and vasopressinergic system may activate the parasympathetic outflows to modulate the signals induced by RWIS

It is well known that the activation of hypothalamic-pituitary-adrenocortical (HPA) axis by stress is an important regulatory mechanism used by most mammals to maintain homeostasis after multiple types of challenges. Whether the activation of OT- and AVP-containing neurons in the PVN and SON in response to the RWIS is dependent on the activation of HPA axis [52]? In the present study, the founding of numerous of Fos-IR nuclei in the PaMP, where corticotropin-releasing hormone (CRF) neurons are messed, seemed to be agreement with this viewpoint.

But our previous study found that in the zona fasciculata of the adrenal cortex, where glucocorticoid was synthesized, no Fos expression was observed during the RWIS. Neuroanatomic studies have shown that hypothalamic OT- and AVP-containing neurons receive neural projections from the NTS and, in turn, send projections to visceral centers in the medullary visceral zone, including the NTS, DMV and spinal cord [53]. Furthermore, bilateral vagotomy attenuated the effect of electric stimulation of the PVN on stress ulcers [23]. In addition, in the present study,

numerous of Fos+OTR-IR and Fos+V$_{1b}$R-IR double labeled neurons were observed in the DMV and NTS. These results support and expend the viewpoint that PVN neurons receive inputs from visceral receptors and then release AVP or OT, part of which project to the NTS or DMV and then activate the parasympathetic outflows [50].

In summary, RWIS for 1 h results in the activations of a large population of OT- and AVP- containing neurons, 31% and 40% in the PVN, 28% and 53% in the SON. In addition, RWIS activates more than 10% of OT and AVP sensitive neurons in the DMV, while lower ratio in the NTS. Thus it is hypothesized that OT- and AVP-containing neurons in the PVN and SON, activated by RWIS, would project to the NTS or DMV, mediated by OTR and V$_{1b}$R, and then the DMV in turn provide the preganglionic efferent fibers to regulate gastric information. But,

up to now, no report has been found to describe that the highest density of OT- and AVP-immunoreactive fibers and the terminals in the DMV and NTS originated in the PVN only or both the PVN and SON. Thus, mechanism of the oxytocinergic and vasopressinergic system during the RWIS needs to be further investigated.

Author Contributions

Conceived and designed the experiments: H-BA. Performed the experiments: D-QZ. Analyzed the data: D-QZ. Contributed reagents/materials/analysis tools: D-QZ. Wrote the paper: D-QZ.

References

1. Garrick T, Buack S, Bass P (1986) Gastric motility is a major factor in cold restraint-induced lesion formation in rats. Am J Physiol Gastrointest Liver Physiol 250(2): 191–9.
2. Ai HB, Zhang ZD (1990) Studies on the mechanism of gastric mucosal injury induced by water-immersion stress in rats. Acta Physiol Sin 42(5): 496–502.
3. Zhang YY, Cao GH, Zhu WX, Cui XY, Ai HB (2009) Comparative study of c-Fos expression in the rat dorsal vagal complex and nucleus ambiguus induced by different durations of restraint water-immersion stress. Chin J Physiol 52(3): 143–150.
4. Zhang YY, Zhu WX, Cao GH, Cui XY, Ai HB (2009) c-Fos expression in the supraoptic nucleus is the most intense during different durations of restraint water-immersion stress in the rat. J Physiol Sci 59(5): 367–75.
5. Travagli RA, Hermann GE, Browning KN, Rogers RC (2006) Brainstem circuits regulationg gastric function. Annu. Rev Physiol 68: 279–305.
6. Cruz MT, Murphy EC, Sahibzada N, Verbalis JG, Gillis RA (2007) A reevaluation of the effects of stimulation of the dorsal motor nucleus of the vagus on gastric motility in the rat. Am J Physiol 292(1): R291–307.
7. Zhou SY, Lu YX, Yao H, Owyang C (2008) Spatial organization of neurons in the dorsal motor nucleus of the vagus synapsing with intragastric cholinergic and nitric oxide/VIP neurons in the rat. Am J Physiol Gastrointest Liver Physiol 294(5): G1201–9.
8. Briski K, Gillen E (2001) Differential distribution of Fos expression within the male rat preoptic area and hypothalamus in response to physical vs. psychological stress. Brain Res Bull 55(3): 401–8.
9. Pacák K, Palkovits M (2001) Stressor specifity of central neuroendocrine responses: implications for stress-related disorders. Endocr Rev 22(4): 502–48.
10. Wang YH, Ai HB, Zhang YY, Cui XY (2007) Effects and mediated pathway of electrical stimulation of nucleus ambiguus on gastric motility and mucus secretion in rats. Scand J Clin Lab Invest 67(5): 489–97.
11. Sun HZ, Zhao SZ, Cui XY, Ai HB (2010) Effects and mechanisms of L-glutamate microinjected into nucleus ambiguus on gastric motility in rats. Chin Med J (Engl) 123(8): 1052–7.
12. Palkovits M (2000) Stress-induced expression of co-localized neuropeptides in hypothalamic and amygdaloid neurons. Eur J Pharmacol 405(1-3): 161–6.
13. Ceccatelli S, Eriksson M, Hökfelt T (1989) Distribution and coexistence of corticotropin-releasing factor-, neurotensin-, enkephalin-, chole-cystokinin-, galanin-, and vasoactive intestinal polypeptide/peptide histidine isoleucine-like peptides in the parvicellular part of the paraventricular nucleus. Neuroendocrinology 49(3): 309–23.
14. Swanson LW, Kuypers HGJM (1980) The paraventricular nucleus of the hypothalamus: cytoarchitectonic subdivisions and organization of projections to the pituitary, dorsal vagal complex, and spinal cord as demonstrated by retrograde fluorescence double-labeling methods. J Comp Neurol 194(3): 555–70.
15. Swaab DF, Nijveldt F, Pool CW (1975) Distribution of oxytocin and vasopressin in the rat supraoptic and paraventricular nucleus. J Endocrinol 67(3): 461–2.
16. George JM, Jacobowitz DM (1975) Localization of vasopressin in discrete areas of the rat hypothalamus. Brain Res 93(3): 363–6.
17. Sofroniew MV, Glasmann W (1981) Golgi-like immunoperoxidase staining of hypothalamic magnocellular neurons that contain vasopressin, oxytocin or neurophysin in the rat. Neuroscience 6(4): 619–43.
18. McCann MJ, Rogers RC (1990) Oxytocin excites gastric-related neurons in rat dorsal vagal complex. J Physiol 428: 95–108.
19. Xiong JJ, Hatton GI (1996) Differential responses of oxytocin and vasopressin neurons to the osmotic and stressful components of hypertonic saline injections: a Fos protein double labeling study. Brain Res 719(1-2): 143–53.
20. Giovannelli L, Shiromani PJ, Jirikowski GF, Bloom FE (1990) Oxytocin neurons in the rat hypothalamus exhibit *c-fos* immunoreactivity upon osmotic stress. Brain Res 531(1-2): 299–303.
21. Giovannelli L, Shiromani PJ, Jirikowski GF, Bloom FE (1992) Expression of *c-fos* protein by immunohistochemically identified oxytocin neurons in the rat hypothalamus upon osmotic stimulation. Brain Res 588(1): 41–8.
22. Miyata S, Itoh T, Lin SH, Ishiyama M, Nakashima T, et al. (1995) Temporal changes of c-*fos* expression in oxytocinergic magnocellular neuroendocrine cells of the rat hypothalamus with restraint stress. Brain Res Bull 37(4): 391–5.
23. Zhang JF, Zheng F (1997) The role of paraventricular nucleus of hypothalamus in stress-ulcer formation in rats. Brain Res 761(2): 203–9.
24. Nishitani S, Moriya T, Kondo Y, Sakuma Y, Shinoharal K (2004) Induction of Fos immunoreactivity in oxytocin neurons in the paraventricular nucleus after female odor exposure in male rats: effects of sexual experience. Cellular and Molecular Neurobiology 24(2): 283–91.
25. Pirnik Z, Mravec B, Kiss A (2004) Fos protein expression in mouse hypothalamic paraventricular (PVN) and supraoptic (SON) nuclei upon osmotic stimulus: colocalization with vasopressin, oxytocin, and tyrosine hydroxylase. Neurochem Int 45(5): 597–607.
26. Pirnik Z, Kiss A (2005) Fos expression variances in mouse hypothalamus upon physical and osmotic stimuli: Co-staining with vasopressin, oxytocin, and tyrosine hydroxylase. Brain Res Bull 65(5): 423–31.
27. Wang LX, Martínez V, Larauche M, Taché Y (2009) Proximal colon distension induces Fos expression in oxytocin-, vasopressin-, CRF- and catecholamines-containing neurons in rat brain. Brain Res 1247: 79–91.
28. Ostrowski NL, Lolait SJ, Bradley DJ, O'Carroll AM, Brownstein MJ, et al. (1992) Distribution of V1a and V2 vasopressin receptor messenger ribonucleic acid in rat liver, kidney, pituitary and brain. Endocrinology 131(1): 533–5.
29. Ostrowski NL, Lolait SJ, Young WS 3rd (1994) Cellular localization of vasopressin V1a receptor messenger ribonucleic acid in adult male rat brain, pineal and brain vasculature. Endocrinology 135(4): 1511–28.
30. Kremarik P, Freund-Mercier MJ, Stoeckel ME (1995) Oxytocin and vasopressin binding sites in the ypothalamus of the rat: histoautoradiographic detection. Brain Res Bul 36(2): 195–203.
31. Barberis C, Tribollet E (1996) Vasopressin and oxytocin receptors in the central nervous system. Crit Rev Neurobiol 10(1): 119–54.
32. Vaccari C, Lolait SJ, Ostrowski NL (1998) Comparative distribution of vasopressin V1b and oxytocin receptor messenger ribonucleic acids in brain. Endocrinology 139(12): 5015–33.
33. Hernando F, Schoots O, Lolait SJ, Burbach JP (2001) Immunohistochemical localization of the vasopressin V1b receptor in the rat brain and pituitary gland: anatomical support for its involvement in the central effects of vasopressin. Endocrinology 142(4): 1659–68.
34. Young WS, Li J, Wersinger SR, Palkovit MR (2006) The vasopressin 1b receptor is prominent in the hippocampal area CA2 where it is unaffected by restraint dtress or adrenalectomy. Neuroscience 143(4): 1031–9.
35. Herrera DG, Robertson HA (1996) Activation of c-fos in the brain. Prog NeuroBiol 50(2-3): 83–107.
36. Zhao DQ, Lu CL, Ai HB (2011) The role of catecholaminergic neurons in the hypothalamus and medullary visceral zone in response to restraint water-immersion stress in rats. J Physio Sci 61(1): 37–45.
37. Zimmermann M (1986) Ethical considerations in relation to pain in animal experimentation. Acta Physiol Scand Suppl 554: 221–33.
38. Paxinos G, Watson C (2005) The rat brain in stereotaxic coordinates, 5th edn. Burlington: Elsevier Academic Press.
39. Bonaz B, Taché Y (1994) Induction of Fos immunoreactivity in the rat brain after cold-restraint induced gastric lesions and fecal excretion. Brain Res 652(1): 56–64.
40. du Plessis I, Mitchell D, Niesler C, Laburn HP (2006) c-Fos immunoreactivity in selected brain regions of rats after heat exposure and pyrogen administration. Brain Res 1120(1): 124–130.
41. Swanson LW, Sawchenko PE (1983) Hypothalamic integration: organization of the paraventricular and supraoptic nuclei. Annu Rev Neuronsci 6: 269–324.

42. Okumura T, Namiki M (1990) Vagal motor neurons innervating the stomach are site-specifically organized in the dorsal motor nucleus of the vagus nerve in rats. J Auton Nerv Syst 29(2): 157–162.

43. Rogers RC, McTigue DM, Herman GE (1996) Vagal control of digestion: modulation by central neural and peripheral endocrine factors. Neurosci Biobehav Rev 20(1): 57–66.

44. Rogers RC, Herman GE, Travagli RA (1999) Brainstem pathways responsible for oesophageal control of gastric motility and tone in the rat. J Physiol 514(Pt2): 369–83.

45. Harrison TA (2001) Chorda tympani nerve stimulation evokes Fos expression in regionally limited neuron populations within the gustatory nucleus of the solitary tract. Brain Res 904(1): 54–66.

46. Krowicki ZK, Burmeister MA, Berthoud HR, Scullion RT, Fuchs K, et al. (2002) Orexins in rat dorsal motor nucleus of the vagus potently stimulate gastric motor function. Am J Physiol 283(2): G465–72.

47. Rinaman L (1998) Oxytocinergic inputs to the nucleus of the solitary tract and dorsal motor nucleus of the vagus in neonatal rats. J Comp Neurol 399(1): 101–9.

48. Michelini LC (2001) Oxytocin in the NTS: a new modulator of cardiovascular control durin gexercise. Ann NY Acad Sci 940: 206–20.

49. Higa KT, Mori E, Viana FF, Morris M, Michelini LC (2002) Baroreflex control of heart rate by oxytocin in the solitary-vagal complex. Am J Physiol Regul Integr Comp Physiol 282(2): R537–45.

50. Benarroch EE (2005) Paraventricular nucleus, stress response, and cardiovascular disease. Clin Auton Res 15(4): 254–63.

51. Rogers RC, Hermann GE (1987) Oxytocin, oxytocinantagonist, TRH, and hypothalamic paraventricular nucleus stimulation effects on gastric motility. Peptides 8(3): 505–13.

52. Volpi S, Rabadan-Diehl C, Aguilera G (2004) Vasopressinergic regulation of the hypothalamic pituitary adrenal axis and stress adaptation. Stress 7(2): 75–83.

53. Sofroniew MW, Weindl A (1980) Identification of parvocellular vasopressin and neurophysin neurons in the suprachiasmatic nucleus of a variety of mammals including primates. J Comp Neurol 193(3): 659–75.